

Investigation of Temperature Dependence of the Irreversibility Line of $\text{GdBa}_2\text{Cu}_3\text{O}_{7-\delta}$ Added with Nanosized Ferrite ZnFe_2O_4

R. Awad · M. Roumié · S. Isber · S. Marhaba ·
A. I. AbouAly · H. Basma

Received: 11 June 2014 / Accepted: 25 August 2014 / Published online: 14 September 2014
© Springer Science+Business Media New York 2014

Abstract Superconducting samples of the type $(\text{ZnFe}_2\text{O}_4)_x\text{GdBa}_2\text{Cu}_3\text{O}_{7-\delta}$ were synthesized by the conventional solid-state reaction technique. The nanosized $(\text{ZnFe}_2\text{O}_4)$ content x varied from 0 to 0.1 wt% of the samples' total mass. The prepared samples were characterized using X-ray powder diffraction (XRD) and scanning and transmission electron microscopes (SEM and TEM). The effect of ZnFe_2O_4 addition, which acts as flux pinning centers, was investigated using ac magnetization at different applied dc magnetic fields. It was found that addition of the nanosized $(\text{ZnFe}_2\text{O}_4)$ up to 0.06 wt% enhances the critical current density J_c and the superconducting transition temperature T_c . On the other hand, the superconducting properties of these samples are deteriorated for $x > 0.06$ wt%. The irreversibility line was thermally activated. The logarithmic plot of H_{irr} versus $(1 - T_{\text{irr}}/T_c(0))$ shows a crossover at about 500 Oe, reflecting the transition from two- to three-dimensional vortex fluctuations. The $B_{\text{irr}}-T$ curves are well fitted according to Matsushita's

model, which is based on the de-pinning mechanism caused by thermally activated flux creep.

Keywords $\text{GdBa}_2\text{Cu}_3\text{O}_{7-\delta}$ · Nanoferrite ZnFe_2O_4 · Ac magnetic susceptibility · Irreversibility field

1 Introduction

Gd-123 is a member of the $\text{REBa}_2\text{Cu}_3\text{O}_{7-\delta}$ high-temperature superconductor family, where RE is rare-earth element. Gd-123 has a remarkable ability of carrying high current, making it an important topic for research [1, 2]. However, its flux pinning capability needs to be improved in order to overcome the rapid decrease in the critical current density J_c with the increase of both temperature and magnetic field. It was shown from previous studies that the addition of nanosized ZrO_2 , SnO_2 , and $(\text{ZrO}_2 + \text{ZnO})$ into bulk superconductor $\text{GdBa}_2\text{Cu}_3\text{O}_{7-\delta}$ enhanced the flux pinning and consequently improved critical current density [3–5], by causing a strong interaction between the flux line networks and the nanosized magnetic particles if the size of these nanoparticles is higher than the coherence length ξ and lower than penetration depth λ . Furthermore, the effect of paramagnetic nanosized ZnFe_2O_4 [6] addition on the microstructure and superconducting transport properties of $(\text{Cu}_{0.5}\text{Tl}_{0.5})$ -1223 was investigated. They found that the incorporation of nanosized ZnFe_2O_4 in $(\text{Cu}_{0.5}\text{Tl}_{0.5})$ -1223 superconductor matrix plays an important role for healing the inter-grain voids, pores, and cracks. On the other side, Gardner et al. [7] studied the effect of Cr paramagnetic impurities in Pd films with applied parallel magnetic fields. They showed an increase in the T_c with the application of parallel magnetic field up to certain doping values of Cr paramagnetic impurities.

R. Awad · S. Marhaba · H. Basma (✉)
Physics Department, Faculty of Science, Beirut Arab University
(BAU), Beirut, Lebanon
e-mail: hadibassma@gmail.com

R. Awad · A. I. AbouAly
Physics Department, Faculty of Science, Alexandria University,
Alexandria, Egypt

M. Roumié
Accelerator Laboratory, Lebanese Atomic Energy Commission,
CNRS, Beirut, Lebanon

S. Isber
Department of Physics, American University of Beirut, PO Box
11-0236, Beirut, Lebanon

H–T diagram of high-temperature superconductors (HTSCS) is considered as an attractive subject in the last few years. The boundary of the H–T plane is called the irreversibility line, separating a magnetically irreversible, zero-resistance state ($J_c \neq 0$) from a reversible region with dissipative properties ($J_c = 0$). The previous studies showed that there is a crossover in dimensionality of the vortex ensemble [8]. At low fields, the vortex lines maintain a 3D character, whereas at high fields, there is a quasi-2D vortex fluctuation.

In this paper, the effect of nanosized ZnFe_2O_4 addition on $\text{GdBa}_2\text{Cu}_3\text{O}_{7-\delta}$ using ac magnetic susceptibility measurements at different applied dc magnetic fields was studied. The irreversibility line was plotted, and the logarithmic plot of B_{irr} versus $(1 - T_{\text{irr}}/T_c(0))$ was studied.

2 Experimental Techniques

Nanosized ZnFe_2O_4 powder was prepared by chemical co-precipitation method. Pure chemical reagents of $\text{FeCl}_3 \cdot 6\text{H}_2\text{O}$ and ZnCl_2 were first dissolved in bi-distilled water, and the Zn/Fe molar ratio was fixed to 1:2. At that point, an alkaline solution (NaOH) was added to the salt solution till the pH was adjusted to 12.5. Then, the solution was heated with continuous stirring at 60 °C for 2 h. Next, the co-precipitated powder was filtered and washed for several times with bi-distilled water and dried in an oven in air atmosphere at 90 °C for 24 h. Finally, the dried powder was calcined in air at 500 °C for 4 h.

Superconducting samples of type $(\text{ZnFe}_2\text{O}_4)_x\text{GdBa}_2\text{Cu}_3\text{O}_{7-\delta}$ $0.0 \leq x \leq 0.1$ wt.%, were prepared by the conventional solid-state reaction technique. First, the starting materials Gd_2O_3 , BaCO_3 , and CuO (purity ≥ 99.9) were crushed in an agate mortar and were sifted using a 125- μm sieve to get a homogeneous mixture. Then, the powder was subjected to calcination process in air at 840 and 880 °C for 24 h each. Next, the resultant powder was ground and sifted, and x wt.% of nanosized ZnFe_2O_4 was added to the resulting powder. At that point, the powder was again mixed for a long time to ensure the homogenous distribution of nanosized ZnFe_2O_4 inside the sample. Subsequently, the mixed powder was pressed in a disk form (1.5 cm in diameter and about 0.3 cm in thickness). Afterwards, disks were sintered in air at 930 °C with a heating rate of 4 °C/min and held at this temperature for 24 h. Then, the samples were cooled by a rate of 1 °C/min down to 450 °C and kept at this temperature for 10 h under oxygen flow to control the oxygen content of the final compounds. Finally, they were slowly cooled by a rate of 1 °C/min to room temperature. The characterization and superconductivity

investigation of these samples was carried out using X-ray powder diffraction (XRD), scanning electron microscopes (SEM), transmission electron microscope (TEM), electrical resistivity, and I–V characteristic [9].

The ac magnetic susceptibility at different applied dc fields was measured using a Quantum Design Physical Properties Measurements System (PPMS) equipped with a 9-T superconducting magnet. The system has a sensitivity of 1×10^{-8} emu, amplitude range of 0.005–15 Oe (peak), and frequency range of 10 Hz–10 KHz, with direct-phase nulling technique that measures and cancels background ac phase shifts at every measurement. The ac magnetic susceptibilities were measured on powder samples of typical masses 200–300 mg at seven different values of the external magnetic fields between 0 and 3,000 Oe. The amplitude of the excitation magnetic field was set to 3 Oe in all runs at a fixed frequency of 1 KHz.

3 Results and Discussions

The analysis of nanosized ZnFe_2O_4 powder by XRD and TEM showed that the crystalline size is around 8 nm [9], while the analysis of superconducting samples showed that relative volume fraction of Gd-123 phase, superconducting transition temperature, and transport critical current density increased as x increased from 0 to 0.06 wt% and a reverse trend was observed for $x > 0.06$ wt% [9].

Figure 1 shows a typical real part of the ac magnetic susceptibility χ' versus temperature curves for $(\text{ZnFe}_2\text{O}_4)_x\text{GdBa}_2\text{Cu}_3\text{O}_{7-\delta}$; $x = 0.00, 0.02, 0.04, 0.06$, and 0.08 wt% at $H = 3$ Oe. The superconducting transition

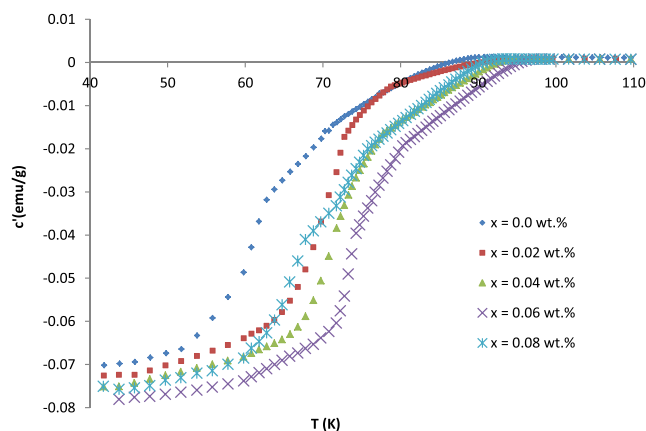


Fig. 1 The real part of the magnetic susceptibility versus temperature at a field of 3 Oe for samples with $x = 0.00, 0.02, 0.04, 0.06$, and 0.08 wt%

Table 1 The values of T_c at $H = 3$ Oe, n_1 of the power relation obtained from (1) at low field ($H < 1,000$ Oe), n_2 of the power relation obtained from (1) at high field ($H > 1,000$ Oe), and the fitting parameters (K , m , and γ) according to (2) for $(\text{ZnFe}_2\text{O}_4)_x\text{GdBa}_2\text{Cu}_3\text{O}_{7-\delta}$; $x = 0.00, 0.04, 0.06,$ and 0.08 wt%

Sample	T_c	n_1	n_2	k	m	γ
Zn-0	89.59	1.43	4.925	85.1	0.0145	1.455
Zn-0.04	93.6	1.46	4.765	86.0	0.0145	1.450
Zn-0.06	95.2	1.53	5.290	91.0	0.0150	1.475
Zn-0.08	91.5	1.58	4.980	90.5	0.0150	1.465

temperature T_c is defined as the temperature at which χ' changes from a positive to a negative value. It is found that T_c increases with the increase of x up to 0.06 wt% and then it decreases with further increases of x . The values of T_c for $x = 0, 0.04, 0.06,$ and 0.08 wt% at $H = 3$ Oe are listed in Table 1. The increase in T_c with x is attributed to the increase in the volume fraction and improves of grain connection of the Gd-123 phase [9], while the decrease in T_c is probably due to the trapping of mobile free carriers and non-uniform distribution of nanoparticles [10] at grain boundaries of the host Gd-123 phase. The magnitude of diamagnetism factor has the highest value for $x = 0.06$ wt% and then it decreases for $x > 0.06$ wt%. As the concentration of the nanosized ZnFe_2O_4 , $x > 0.06$ wt%, gets higher, the composition at the termination ends of the crystal may be altered. Subsequently, this will increase the normal-state resistivity of the material and the inadvertent phase formation at the termination ends of the crystal. Thus, the formation of this phase would suppress the magnitude of the diamagnetism of the final compound [11]. On the other hand, the Gd-123 samples show different behaviors where the intrinsic component of χ' shows much stronger effect to the applied field [12]. This behavior is due to the response of χ' to the applied field just below the transition temperature T_c , where the intrinsic (grain) component arises. Namuco et al. [13] compared between the ac magnetic susceptibility of Y-123 and Gd-123, and the results revealed that Gd-123 showed a more sensitive ac magnetic susceptibility

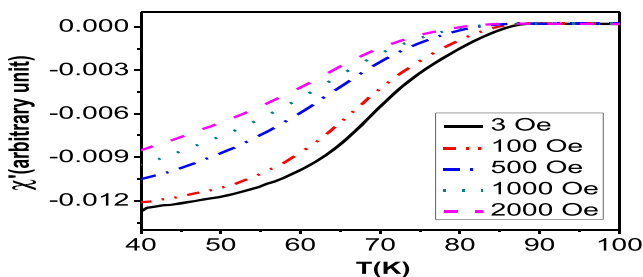


Fig. 2 The real part of the magnetic susceptibility for $(\text{ZnFe}_2\text{O}_4)_{0.1}\text{GdBa}_2\text{Cu}_3\text{O}_{7-\delta}$ versus temperature at different applied dc fields

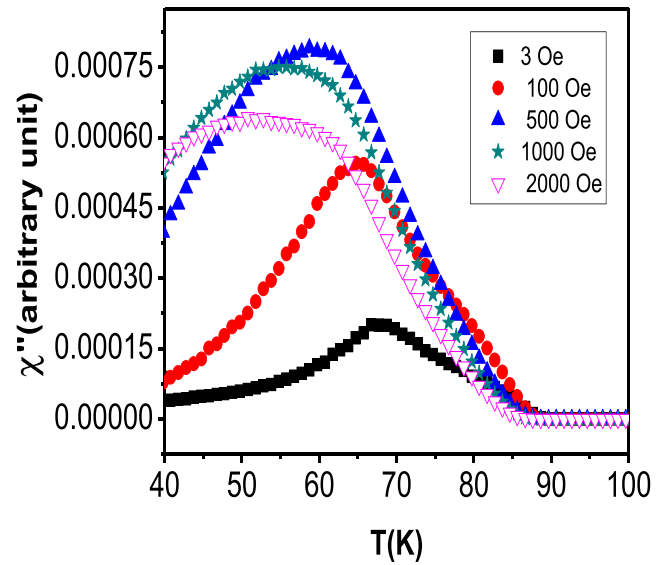


Fig. 3 The imaginary part of the magnetic susceptibility for $(\text{ZnFe}_2\text{O}_4)_{0.1}\text{GdBa}_2\text{Cu}_3\text{O}_{7-\delta}$ versus temperature at different applied dc fields

response. Figure 2 shows the real part of the ac magnetic susceptibility of the sample $(\text{ZnFe}_2\text{O}_4)_{0.1}\text{GdBa}_2\text{Cu}_3\text{O}_{7-\delta}$ at different applied dc magnetic fields. It is clear that the diamagnetic temperature shifted to lower values as the applied dc magnetic field increases. Figure 3 shows the imaginary part of the ac magnetic susceptibility of the sample $(\text{ZnFe}_2\text{O}_4)_{0.1}\text{GdBa}_2\text{Cu}_3\text{O}_{7-\delta}$. The χ'' curves of our samples have only one peak, indicating that these samples have no or small separation between the intragrain and the dissipative inter-grain transition. This means that the applied dc magnetic field is not sufficient to penetrate the intragrain superconductors, signifying good electrical contacts between the superconducting grains. These results are consistent with those obtained by Chen et al. [14] for (Bi,

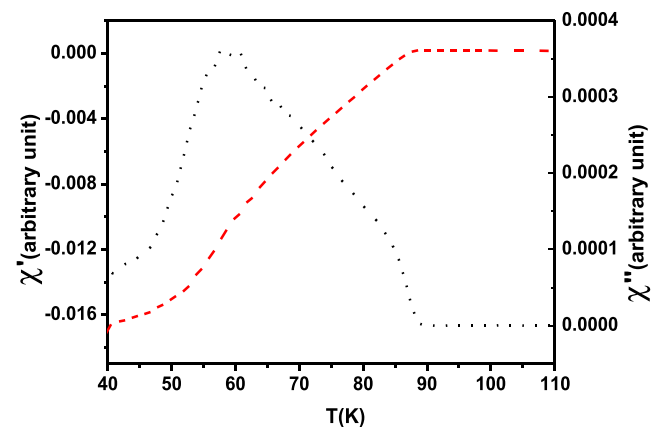


Fig. 4 The temperature dependence of the real (right) and imaginary (left) magnetic susceptibility for the sample $(\text{ZnFe}_2\text{O}_4)_{0.06}\text{GdBa}_2\text{Cu}_3\text{O}_{7-\delta}$ at a field $H = 3$ Oe

Pb)-2223 sintered samples and are in contrast to the situation found for Tl-2201 and Bi-2212 ceramics [15]. The peak of χ'' (at T_p) increases with the applied magnetic field up to $H = 500$ Oe, indicating maximum losses caused by the motion of inter-granular Josephson coupling. This peak decreases for $1,000 \text{ Oe} \leq H \leq 3,000$ Oe. Figure 4 shows the temperature dependence of the real and imaginary parts of the ac magnetic susceptibility χ' and χ'' for the $(\text{ZnFe}_2\text{O}_4)_{0.06}\text{GdBa}_2\text{Cu}_3\text{O}_{7-\delta}$ compound. It is noticed that $\chi''_{ac}(T)$ shows a peak which coincides with the inflection point in $\chi'_{ac}(T)$ curve.

The irreversibility temperature (T_{irr}) is defined as the temperature at which χ'' is maximum in the presence of a certain applied magnetic field. The irreversibility line (IL) shows a dimensional crossover from a 3D vortex state at low magnetic fields to a 2D vortex state at high magnetic fields. This crossover usually refers as the melting of the vortices and it is shown from the graphs regardless of the position of the IL. The crossover always occur at the same field ($H_{dc} = 500$ Oe). Figure 5 shows the logarithmic plot between the applied magnetic field H_{irr} and $(1 - T_{irr}/T_0)$ for $(\text{ZnFe}_2\text{O}_4)_x\text{GdBa}_2\text{Cu}_3\text{O}_{7-\delta}$ compounds with $x = 0.04$, $x = 0.06$, and $x = 0.08$ wt%. The experimental data are well fitted according to the relation

$$H_{irr} = [1 - T_{irr}/T_0]^n, \quad (1)$$

where the value of n varies from one HTSC family to another and is usually between 1.5 and 5.5. This is related to the degree of anisotropy of the system [16]. The values of n_1 (for $H < 1,000$ Oe) and n_2 (for $H \geq 1,000$ Oe), obtained from fitting of the experimental data according to (1), are listed in Table 1. The values of n_1 and n_2 are consistent with those obtained by Chan et al. for the phase $\text{Tl}_2\text{Ba}_2\text{Ca}_2\text{Cu}_3\text{O}_{10\pm\delta}$ [17–20]. The proposed theoretical interpretation for the nature of H_{irr} includes thermal de-pinning [16] and vortex glass transition [21]. The exponential dependence of T_{irr} at low fields is interpreted in

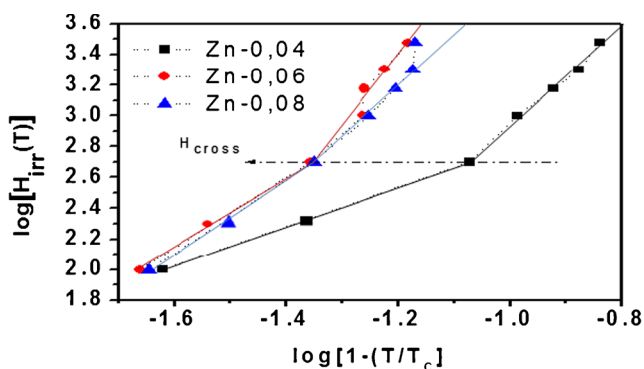


Fig. 5 Log (H_{irr}) versus $\log(1 - T/T_c)$ for $(\text{ZnFe}_2\text{O}_4)_x\text{GdBa}_2\text{Cu}_3\text{O}_{7-\delta}$ with $x = 0.04$, 0.06 , and 0.08 wt%

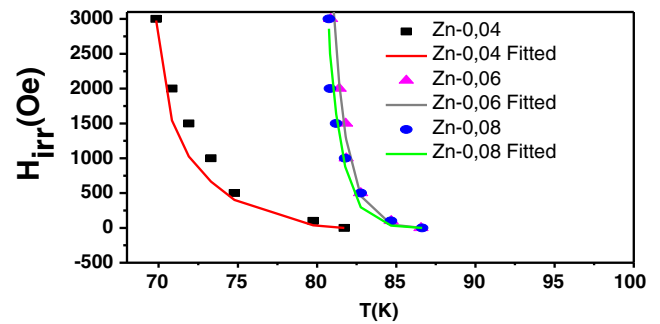


Fig. 6 Fitting of H_{irr} versus T by Matsushita's formula for $(\text{ZnFe}_2\text{O}_4)_x\text{GdBa}_2\text{Cu}_3\text{O}_{7-\delta}$ with $x = 0.04$, 0.06 , and 0.08 wt%

terms of thermal de-pinning [22]. At higher fields, H_{irr} is explained in terms of a thermally activated 3D–2D crossover [23] and glass transition [24].

Matsushita [25, 26] introduced a model based on a de-pinning mechanism caused by thermally activated flux creep which is expressed by the following equation:

$$H_{irr} = \left(\frac{K}{T}\right)^{\frac{4}{3-2\gamma}} \left[1 - \left(\frac{T}{T_c}\right)^2\right]^{\frac{2m}{3-2\gamma}}, \quad (2)$$

where K , m , and γ are numerical parameters of the theory dependent on the creep free pinning force and current density. The experimental result with the fitting according to (2) for $(\text{ZnFe}_2\text{O}_4)_x\text{GdBa}_2\text{Cu}_3\text{O}_{7-\delta}$ compounds with $x = 0.04$, $x = 0.06$, and $x = 0.08$ wt%; and the fitted data are shown in Fig. 6. It is clear that the experimental results are well fitted to (2) with the best parameters K , m , and γ , which are listed in Table 1.

4 Conclusions

The effect of dc magnetic fields up to 3,000 Oe on $(\text{ZnFe}_2\text{O}_4)_x\text{GdBa}_2\text{Cu}_3\text{O}_{7-\delta}$ has been studied. It was found that the addition of the nanosized $(\text{ZnFe}_2\text{O}_4)_x$ increased the superconducting transition temperature up to $x = 0.06$ wt% and then it decreased with further increase of x . The logarithmic plots of H_{irr} versus $(1 - T_{irr}/T_c)$ showed a crossover at a field (H_{dc}) = 500 Oe, reflecting a transition from 2D to 3D vortex fluctuations. Moreover, the H_{irr} – T curves are well fitted with Matsushita's formula, indicating a thermally activated flux creep behavior.

Acknowledgments This work was performed in the superconductivity and metallic-glass lab, Faculty of Science, Alexandria University, EGYPT and in Collaboration with SI, Physics Department at American University of Beirut, Beirut, Lebanon.

References

1. Zhang, Y.F., Izumi, M., Li, Y.J., Murakami, M., Gao, T., Liu, Y.S., Li, P.L.: *J. Phys. C* **47**, 1840 (2011)
2. Sakai, N., Lee, S., Chikumoto, N., Izumi, T., Tanabe, K.: *J. Phys. C* **471**, 1075 (2011)
3. Xu, C., Hu, A., Ichihara, M., Sakai, N., Hirabayashi, I., Izumi, M.: *J. Phys. C* **460–462**, 1341 (2007)
4. Xu, C., Hu, A., Sakai, N., Izumi, M., Hirabayashi, I.: *J. Phys. C* **357**, 445–448 (2006)
5. Xu, Y., Hu, A., Xu, C., Sakai, N., Hirabayashi, I., Izumi, M.: *Phys. J. C* **468**, 1363 (2008)
6. Mumtaz, M., Naeem, S., Nadeem, K., Naeem, F., Jabbar, A., Zheng, Y.R., Khan, N.A., Imran, M.: *J. Solid State Sci.* **22**, 21 (2013)
7. Gardner, H.J., Kumar, A., Yu, L., Xiong, P., Warusawithana, M.P., Wang, L., Vafek, O., Schlom, D.G.: *J. Nat. Phys.* **7**, 895 (2011)
8. Schilling, A., Jin, R., Guo, J.D., Ott, H.R.: *J. Phys. Rev. Lett.* **71**, 1899 (1993)
9. Abou Aly, A.I., Awad, R., Isber, S., Mohammed, N.H., Motaweh, H.A., El-Said Bakeer, D.: *J. Alloys Compd.* (2014). (accepted)
10. Khan, N.A., Mumtaz, M., Ullah, A., Hassan, N., Khurram, A.A. *J. Alloys Compd.* **507**, 142 (2010)
11. Khan, N.A., Saleem, A., Hussain, S.T.: *J. Supercond. Nov. Magn.* **25**, 1725 (2012)
12. Bahgat, A.A., Shaisha, E.E., Saber, M.M.: *J. Phys. B* **399**, 70 (2007)
13. Namuco, S.B., Lao, M.L., Sarmago, R.V.: *J. Phys. Procedia.* **45**, 169 (2013)
14. Chen, D.X., Mei, Y., Luo, H.L.: *J. Phys. C* **167**, 317 (1990)
15. Mezzetti, E., Gerbaldo, G., Ghigo, G., Gozzelino, L., Minetti, B.: *J. Phys. Rev. B* **60**, 7623 (1999)
16. Yeshurn, Y., Malozemoff, A.: *J. Phys. Rev. Lett.* **60**, 2202 (1987)
17. Chan, K., Liou, S.H.: *Phys. J. Rev. B* **45**, 5547 (1992)
18. Huang, Z., Xue, Y., Meng, R., Chu, C.: *J. Phys. Rev. B* **49**, 4218 (1994)
19. Xu, W., Suenaga, O.: *J. Phys. Rev. B* **43**, 5516 (1991)
20. Estrela, P., Abilio, C., Godinho, M., Tholence, J.L., Capponi, J.J.: *J. Phys. C* **235–240**, 2731 (1994)
21. Fisher, M.P.A.: *J. Phys. Rev. Lett.* **62**, 1415 (1989)
22. Miu, L.: *Phys. J. Rev. B* **46**, 1172 (1992)
23. Kim, D.H., Gray, K.E., Kampwirth, R.T., Smith, J.C., Richardson, T.J., Kang, J.H., Talvacchio, J., Eddy, M.: *J. Phys. C* **177**, 431 (1991)
24. Safar, H., Gammel, P.L., Bishop, D.: *J. Phys. Rev. Lett.* **68**, 2672 (1992)
25. Matsushita, T.: *J. Phys. C* **205**, 289 (1993)
26. Matsushita, T.: *J. Phys. C* **164**, 150 (1990)